Received: 7 July 2021 | Revised: 21 March 2022 | Accepted: 3 April 2022

DOI: 10.1002/jez.b.23137

RESEARCH ARTICLE

JEZ-B MOLECULAR AND DEVELOPMENTAL EVOLUTION WILEY

The nested embryonic dorsal domains of BMP-target genes are not scaled to size during the evolution of *Drosophila* species

Juan Sebastian Chahda[1] | Priscilla Ambrosi[1] | Claudia M. Mizutani[1,2]

[1]Department of Biology, College of Arts and Sciences, Case Western Reserve University, Cleveland, Ohio, USA

[2]Department of Genetics and Genome Sciences, School of Medicine, Case Western Reserve University, Cleveland, Ohio, USA

Correspondence

Claudia M. Mizutani, Department of Biology, College of Arts and Sciences, Case Western Reserve University, Cleveland, OH, USA.
Email: claudia.mizutani@case.edu

Funding information

National Science Foundation, Grant/Award Number: IOS-1051662; National Institutes of Health, Grant/Award Numbers: R21EB016535, R33AG049863

Abstract

Egg size is a fast-evolving trait among Drosophilids expected to change the spatial distribution of morphogens that pattern the embryonic axes. Here we asked whether the patterning of the dorsal region of the embryo by the Decapentaplegic/Bone Morphogenetic Protein-4 (DPP/BMP-4) gradient is scaled among *Drosophila* species with different egg sizes. This region specifies the extra-embryonic tissue amnioserosa and the ectoderm. We find that the entire dorsal region scales with embryo size, but the gene expression patterns regulated by DPP are not proportional, suggesting that the DPP gradient is differentially scaled during evolution. To further test whether the DPP gradient can scale or not in *Drosophila melanogaster*, we created embryos with expanded dorsal regions that mimic changes in scale seen in other species and measured the resulting domains of DPP-target genes. We find that the proportions of these domains are not maintained, suggesting that the DPP gradient is unable to scale in the embryo. These and previous findings suggest that the embryonic dorso-ventral patterning lack scaling in the ventral and dorsal sides but is robust in the lateral region where the neuroectoderm is specified and two opposing gradients, Dorsal/NFkappa-B and DPP, intersect. We propose that the lack of scaling of the DPP gradient may contribute to changes in the size of the amnioserosa and the numbers of ectodermal cells with specific cortical tensions, which are expected to generate distinct mechanical forces for gastrulating embryos of different sizes.

KEYWORDS

amnioserosa, dorso-ventral patterning, DPP/BMP-4 gradient, *Drosophila* species, ectoderm, embryogenesis, evolution of development, gastrulation, gene regulation, scaling of morphogenetic gradients

1 | INTRODUCTION

Egg size is a remarkably fast evolving trait observed in *Drosophila* species (Ambrosi et al., 2014; Belu & Mizutani, 2011; Chahda et al., 2013; Crocker et al., 2008; Garcia et al., 2013; Gregor et al., 2005; Lott et al., 2007; Markow et al., 2009; Umulis et al., 2010). Changes in embryo size are expected to cause redistribution of morphogenetic gradients that specify the ventral mesoderm, lateral neuroectoderm, and dorsal ectoderm along the dorso-ventral (DV) axis (Mizutani & Bier, 2008; Schloop et al., 2020; Stathopoulos & Levine, 2002, 2005). Previously, we showed that the constancy in the size of the neuroectodermal domain, a hallmark across divergent insect species that share stereotyped neural lineages (Doe, 1992; Thomas et al., 1984; Whitington, 1996), is achieved through variations in mesodermal size among species with small and large eggs (Ambrosi et al., 2014; Chahda et al., 2013). In four species analyzed, *Drosophila melanogaster* and *Drosophila simulans* (similar egg sizes), *Drosophila sechellia* (large egg size) and *Drosophila busckii* (small egg size), we find differences in the shape of the maternal Dorsal (DL)/NFkappaB gradient (Ambrosi et al., 2014; Chahda et al., 2013), responsible for DV patterning (Reeves & Stathopoulos, 2009; Stathopoulos & Levine, 2002). These species-specific DL gradient shapes cause an expansion or retraction of the mesoderm, leading to the repositioning of the ventral border of the neuroectoderm. Cells at the repositioned border have equal levels of DL and Decapentaplegic (DPP)/Bone Morphogenetic Protein-4 (BMP-4) across the different species, allowing for the specification of conserved expression domains of neural identity genes (Ambrosi et al., 2014; Chahda et al., 2013; Mizutani et al., 2006). In these species, the stereotyped array of abdominal muscles is not affected by the enlargement or shrinkage of the mesoderm due to a compensatory mechanism that changes the rate of myoblast fusions (Belu & Mizutani, 2011).

Although the studies above revealed a mechanism that preserves the neuroectodermal size and neuronal lineages across species by shrinking or expanding the mesoderm, the effects of embryo size on the dorsal region remain largely unknown. In this region, the DPP gradient establishes nested domains of gene expression that specify the ectoderm and the amnioserosa. Currently, it is not known whether the DPP gradient and the expression domains of DPP-target genes are scaled to embryo size during evolution. Previous work showed that the DPP/BMP gradient scales to size in other developmental contexts. For example, during growth of *Drosophila* wing disks, bisected *Xenopus* embryos, and *zebrafish* pectoral fin patterning (Ben-Zvi et al., 2008; Hamaratoglu et al., 2011; Mateus et al., 2020). A model of "expansion-repression integral feedback control" proposes that a molecule secreted far from the morphogen source functions as an "expander" by interacting with the morphogen and increasing its spread in the extracellular domain. The expansion of the gradient is then balanced by a cross-regulation between the expander and the morphogen itself (Ben-Zvi, Shilo, et al., 2011). The proteins Pentagone (PENT)/MAGU and SMOC1 have been shown to act as an expander of the DPP/BMP gradients in the *Drosophila* wing and *zebrafish* fin, respectively (Ben-Zvi, Pyrowolakis, et al., 2011; Hamaratoglu et al., 2011; Mateus et al., 2020). *pent/magu* is expressed at moderate levels in the *Drosophila* embryo (Graveley et al., 2011), but it is not known whether it may contribute to scaling the DPP gradient.

Potential differences in the patterning of the dorsal region of these *Drosophila* species may reveal important adaptions to support the gastrulation of embryos of varying sizes and determine the speed of embryogenesis (Huang & Umulis, 2019; Kuntz & Eisen, 2014; Markow et al., 2009). The amnioserosa and ectodermal cells have unique mechanical properties essential for the major morphogenetic movements that occur during gastrulation (Gorfinkiel et al., 2011; Kong et al., 2017; Lacy & Hutson, 2016). The amnioserosa derives from dorsal most cells exposed to peak DPP levels and actively participate in germ band extension, retraction, and dorsal closure by creating mechanical forces in the adjacent epidermis (Gorfinkiel et al., 2011; Kong et al., 2017; Lacy & Hutson, 2016). For example, mutant embryos for the DPP-target genes belonging to the u-shaped group (e.g., u-shaped, hindsight, tailup) have reduced or no amnioserosal tissue and cannot retract their germ band. Similarly, the mesoderm invagination creates tensile forces along the AP axis that are important for the germ band extension (Butler et al., 2009). Another study showed that cell cortical tension forces are variable along the DV axis and are required for the mesoderm invagination (Rauzi et al., 2015). Indeed, the immobilization of a stripe of cells located in the ectoderm can abrogate mesodermal invagination (Rauzi et al., 2015), indicating that ectodermal cells can regulate morphogenetic movements that happen far away in the mesoderm. If the expression domains of DPP-target genes are not scaled to embryo size, then cells in similar DV positions in the different species are expected to provide distinct mechanical forces for gastrulating embryos of different sizes. Thus, to understand species-specific differences in the timescale of gastrulation and embryonic development as a whole, it is fundamental to determine whether or not the DPP gradient is scaled to size and how amnioserosal and ectodermal cell fates are specified during evolution.

Together the findings above highlight the importance of the DPP gradient in creating cell territories that possess distinct mechanical properties required for gastrulation. Here we asked if the expression domains of DPP-target genes are scaled to size or are skewed in species with embryos of different sizes. We find that the expression domains established by varying DPP levels do not maintain proportionality across species, particularly in the presumptive amnioserosa. In addition, we manipulated *D. melanogaster* embryos and show that the DPP gradient does not scale in response to an expanded ectoderm. Our results suggest that the evolutionary scaling of the DPP gradient does not exert a uniform effect across its target genes.

2 | RESULTS

2.1 | The entire dorsal embryonic domain scales with embryo size

To test whether the expression domains of DPP-target genes are affected by embryo size, we analyzed the following *Drosophila* species with morphologically distinct embryos: *D. melanogaster* and its sibling species *D. simulans* and *D. sechellia;* and a more divergent species *D. busckii*, *D. simulans*, and *D. sechellia* diverged 0.3–0.5 MYA from each other, and roughly 5–6 MYA from *D. melanogaster* (Figure 1a) (David et al., 2007; Lachaise et al., 1986; Tamura et al., 2004). Despite these short divergence times, *D. sechellia* has evolved much larger embryos than its sibling species (Belu & Mizutani, 2011; Chahda et al., 2013; Lott et al., 2007; Markow et al., 2009) (Figure 1a). *D. busckii* produces the smallest embryos studied here (Belu & Mizutani, 2011; Chahda et al., 2013; Gregor et al., 2005), and diverged from *D. melanogaster* an estimated 50 MYA (Figure 1a). We previously showed that the total number of nuclei along the DV axis in the species above is variable and correlates with embryo size, whereas the neuroectoderm has a conserved size (Chahda et al., 2013).

We found that the entire dorsal region scales with embryo size in these species, as seen by the absolute numbers and relative percentage of nuclei expressing *dpp* along the DV axis within the center most region of the embryo (Figure 1b–d). Our results show that *D. busckii* has the smallest numbers of *dpp*+ cells, followed by *D. simulans* and *D. melanogaster* (Figure 1b). Finally, *D. sechellia* displays the largest numbers of *dpp*+ cells. Thus, the dorsal embryonic region scales to the embryo sizes of these species and maintain a proportional percentage of 40% out of the total numbers of DV nuclei (Figure 1c). We note that in *D. melanogaster*, there is a slight increase from 40% to 43%.

2.2 | The relative range of peak DPP activity is inversely correlated with embryo size

We next asked if the DPP activity gradient established within the dorsal region also scales to size. We measured the levels of phosphorylated mothers against dpp (pMAD), the intracellular transducer of DPP signaling that can be used as a direct read-out of peak DPP levels (Newfeld et al., 1996; Wotton & Massagué, 2001). In *D. melanogaster*, the pMAD signal initially appears weak and diffuse, but quickly sharpens and increases in intensity by mid- to late-blastoderm stage, forming a thin stripe along the dorsal midline in response to peak DPP activity (Dorfman & Shilo, 2001; Maduzia & Padgett, 1997; Mizutani & Bier, 2008; Raftery & Sutherland, 1999; Sutherland et al., 2003). In the species analyzed here, pMAD also forms a thin and intense stripe along the dorsal midline by late

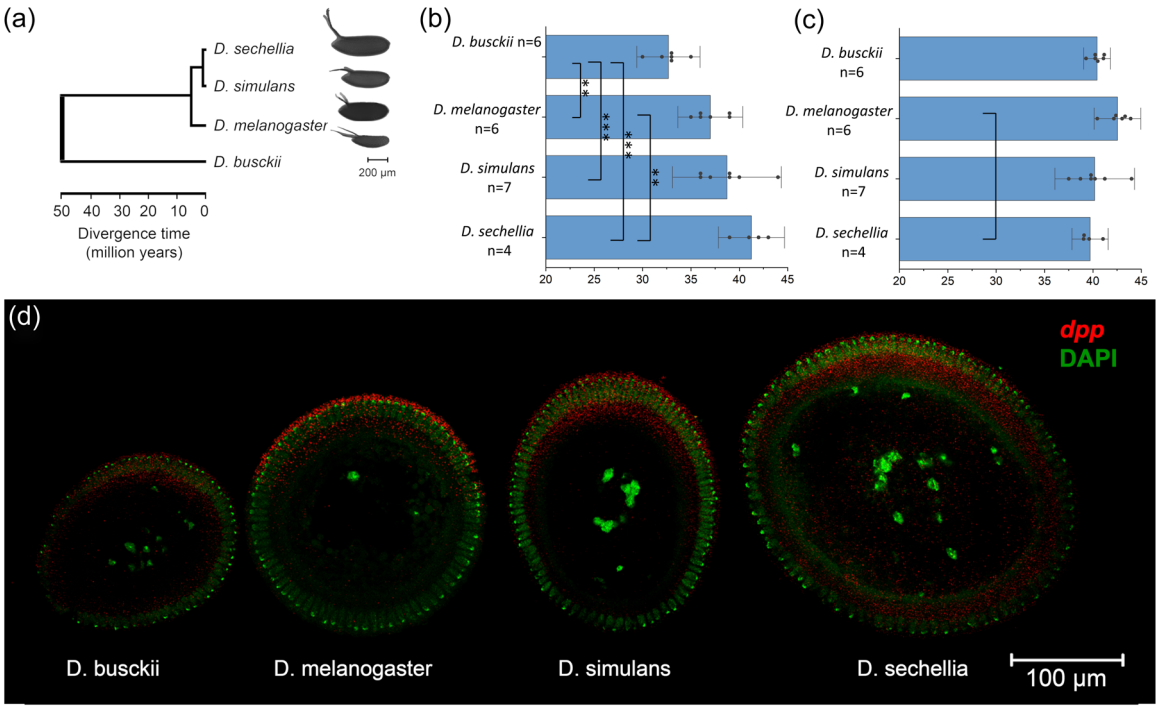

FIGURE 1 The relative size of the ectoderm ranges from 40% to 43% across species that produce embryos of different sizes. (a) Phylogenetic tree of *Drosophila* sibling species (*melanogaster* subgroup) and *Drosophila busckii.* Lateral view of embryos produced by these species showing their different sizes (scale bar, 200 µm). (b) The average number of cells expressing *dpp* along the dorsal-ventral axis. (c) The percent of *dpp* expressing cells in relation to the total numbers of cells along the DV axis. Error bars are 2 standard deviations in both directions. NS, not significant. $*p < 0.05$, $**p < 0.01$, $***p < 0.001$. (d) Cross sections of blastoderm stage embryos across species. Embryos are stained against *dpp* RNA (red) and nuclear dye DAPI (green). Ventral is down

blastoderm stage (Figure 2a). Next, we asked if there were differences in the distribution of pMAD in these species by normalizing the intensity levels of nuclear pMAD across 15 nuclei along the DV axis (Figure 2b) and determining the number of nuclei with peak pMAD levels at or above 50% maximum intensity (dotted line in Figure 2b). These analyses show that the distribution and range of pMAD is similar in *D. melanogaster* and *D. simulans* (Figure 2b), which is consistent with the fact that these species have their embryos of similar size and numbers of *dpp*+ cells. In contrast, in the small *D. busckii* embryos, the levels of pMAD have a sharper decrease than *D. melanogaster* and the number of cells experiencing peak DPP activity is two cells fewer than *D. melanogaster* and *D. simulans* (Figure 2b). The large *D. sechellia* embryos shows a wider pMAD distribution with two cells more than *D. melanogaster* and *D. simulans* (Figure 2b). By fitting the pMAD intensity level plots to Gaussian curves, we calculated the values of full width at half maximum (FWMH). In agreement with the observations above, the calculated FWHM are similar between *D. melanogaster* and *D. simulans* (5.19335 and 5.60499, respectively), smaller in *D. busckii* (4.99631) and larger in *D. sechellia* (7.33353).

Even though the pMAD domain increases in concert with the domain expressing *dpp*, the ratio between these two domains is not scaled in the different species. In fact, we find an inverse correlation between peak DPP activity (pMAD domain) and the dorsal region of the embryo (*dpp* expressing cells) (R^2 value of 0.87) (Figure 2c). For example, *D. busckii* has the largest range of peak DPP activity, whereas *D. sechellia* has the smallest range of peak DPP activity, despite the fact these species have the smallest and largest ectoderm and overall embryo sizes, respectively. These results suggest that the DPP gradient assumes different shapes across species. If this is the

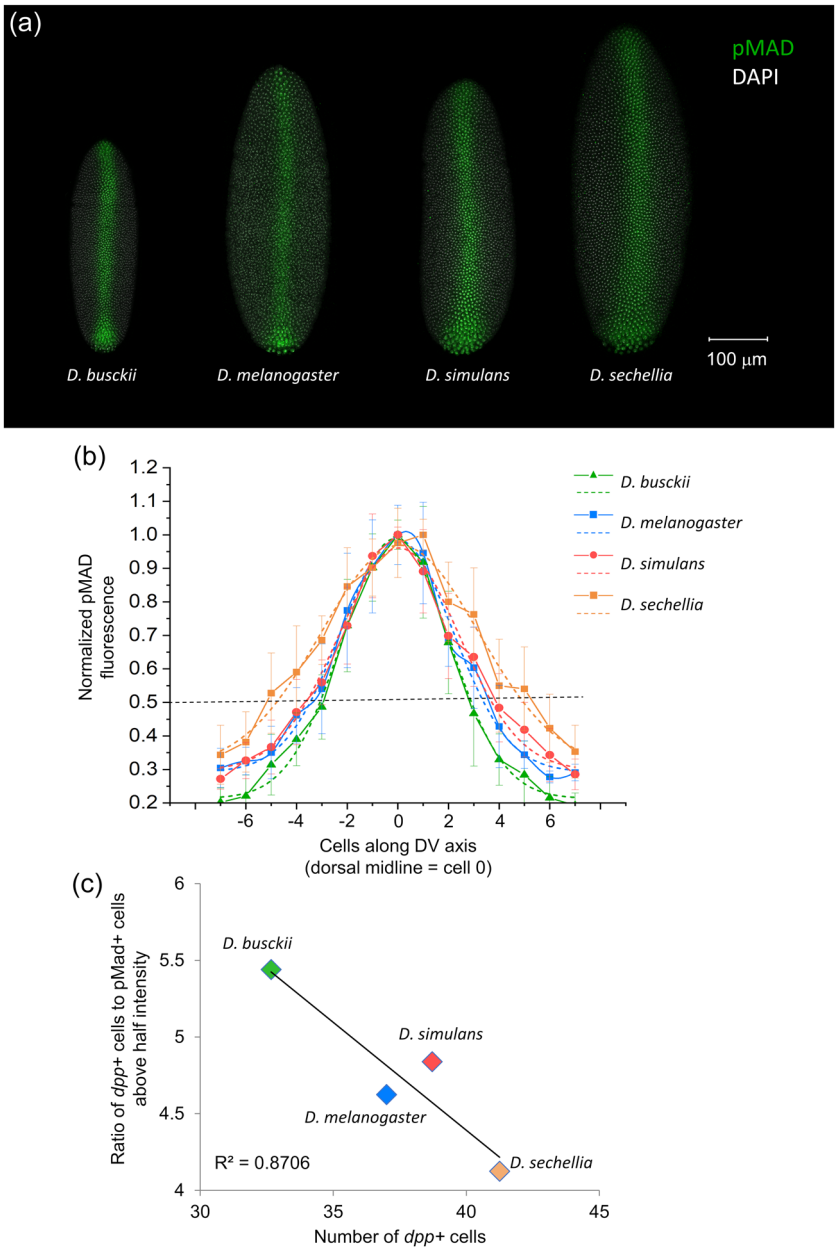

FIGURE 2 The range of peak Decapentaplegic (DPP) activity does not scale to embryo size. (a) phosphorylated mothers against dpp (pMAD) staining across species. Posterior is down. (b) Normalized pMAD distributions across species for the 15 dorsal most cells. Solid line, normalized pMAD intensity level averages; dotted line, Gaussian curve fits. The black dotted line represents the demarcation for the half max pMAD intensity used to determine the number of cells experiencing peak DPP activity in (c). Error bars are 1 standard deviation in both directions. (c) The ratio between cells expressing *dpp* and cells experiencing ≥half max pMAD intensity, plotted against the number of cells expressing *dpp*. DV, dorsal-ventral

case, the expression domains of DPP-target genes defined by additonal DPP threshold levels should display changes in size in the different species.

2.3 | Expression domains of DPP-target genes do not scale with *dpp* expression domain

To test the possibility that the expression of DPP-target genes are changed across the different species, we quantified the expression domain widths for *zerknult* (*zen*), *rhomboid* (*rho*), and *pannier* (*pnr*) within the embryo trunk region (Figure 3a). These genes are activated by peak, high, and moderate threshold levels of DPP, respectively (Ashe et al., 2000; Jaźwińska et al., 1999; Rushlow et al., 2001; Winick et al., 1993). We note that *rho* is expressed in a dorsal stripe, which was measured here, as well as in ventral stripes corresponding to the neuroectoderm (Bier et al., 1990). Finally, the region receiving the lowest levels of DPP gradient in the ventral ectoderm can be estimated by counting the number of cells that express *dpp* but not *pnr*. In contrast to pMAD measurement as a direct read-out of peak levels of the DPP gradient, assaying for the expression of DPP-target genes is an indirect method that does not account for potential modifications in the *cis*-regulatory responses of DPP-target gene enhancers that may have occurred during evolution. Nonetheless, this approach allows us to analyze regions of moderate and low concentration levels of the DPP gradient and it reveals the final

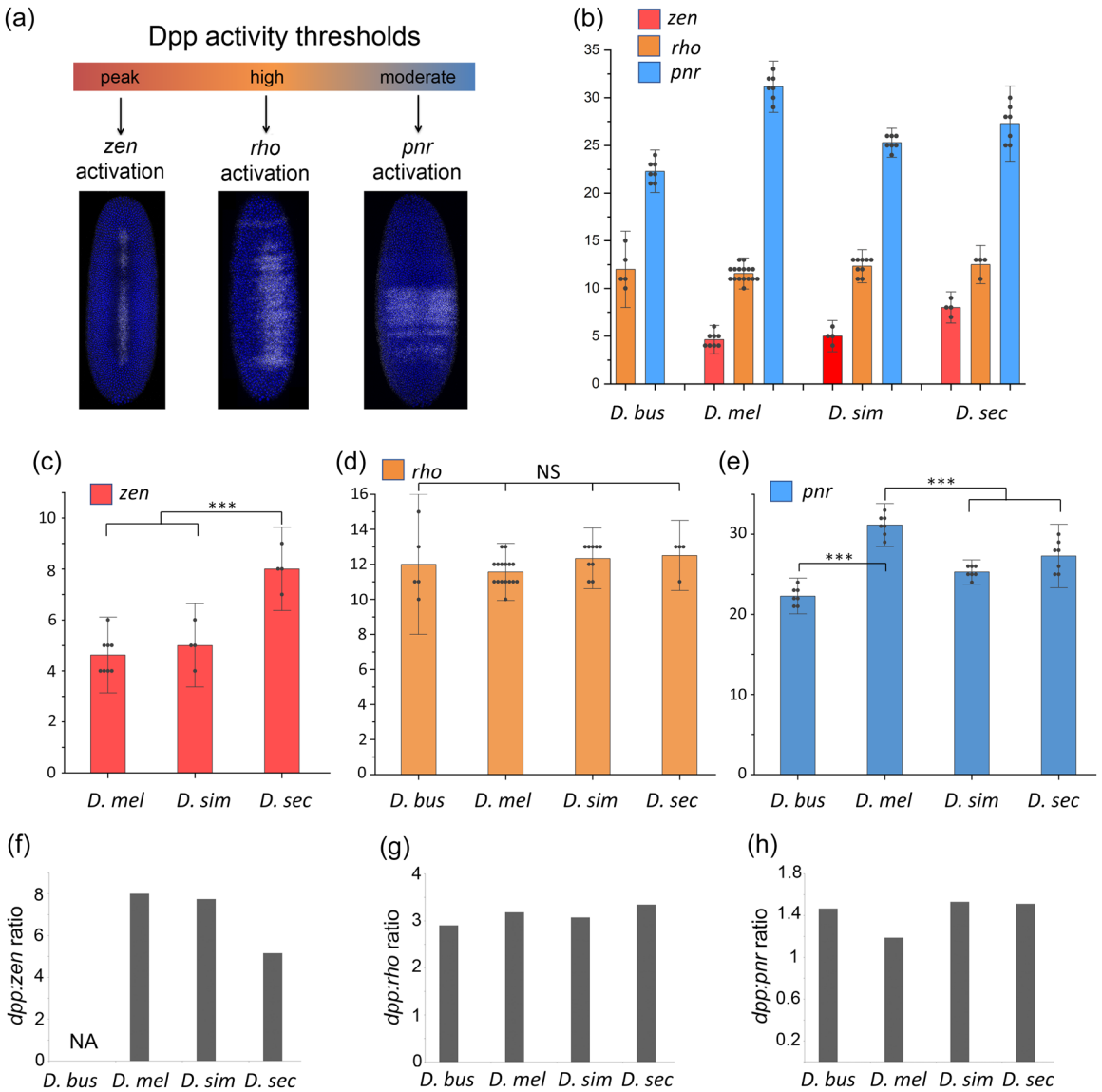

FIGURE 3 The expression domains of Decapentaplegic (DPP)-target genes are not proportional and do not scale with the total expression domain of *dpp*. (a) The DPP target genes *zen*, *rho*, and *pnr* have different activation thresholds and are used as a readout of DPP activity. Dorsal views of blastoderm embryos stained for DPP target genes. Posterior is down. Number of cells expressing *zen* (b, c), *rho* (b, d), and *pnr* (b, e) along the DV axis across species. Error bars are 2 standard deviation in both directions. (f–h) Ratios of *dpp* to *zen*; *dpp* to *rho*; and *dpp* to *pnr* expression widths. $^{*}p < 0.05$; $^{**}p < 0.01$, $^{***}p < 0.001$

evolutionary outcome of ectodermal and amnioserosal patterning in eggs of variable sizes.

zen specifies the amnioserosa (Rushlow et al., 2001). Changes that increase or decrease the *zen* domains in these species would increase or decrease the size of the amnioserosa, an extra-embryonic tissue that is required for gastrulation (Lacy & Hutson, 2016). In addition, *zen* and *rho* specify cells with a higher elasticity that must stretch to allow the more rigid lateral cells to move as a block towards the ventral furrow during mesodermal invagination (Rauzi et al., 2015). Thus, changes in *zen* and *rho* domains would increase or decrease the number of these elastic cells and change the mechanical forces required for mesodermal invagination. Finally, we also selected *pnr* for these analyses, since its expression border falls within the transition region between elastic cells located dorsally and rigid cells laterally. When cells at this position (approximately 45° of embryonic circumference [Jaźwińska et al., 1999]) are immobilized, the mesodermal invagination does not occur because the dorsal cells become unable to stretch to allow the more rigid lateral cells to move ventrally (Rauzi et al., 2015). Thus, by measuring *pnr* domains in these species we can test whether this border moved to a new position.

Similarly to *D. melanogaster*, the sibling species *D. simulans* and *D. sechellia* show a complete refinement of *zen* expression from a broad domain (regulated by DL) to a sharp domain in response to peak DPP levels, matching their pMAD stripes (Figure 3a–c) (Jaźwińska et al., 1999; Rushlow et al., 2001). *D. melanogaster* and *D. simulans* share a *zen* domain of same width at five cells (Figure 3b,c), whereas *D. sechellia* has a wider *zen* expression domain at eight cells (Figure 3b,c). Thus, these experiments show that *D. sechellia* specify a larger amnioserosa, which is consistent with a likely requirement of stronger mechanical forces to sustain the gastrulation of its larger embryo. The *zen* expansion in *D. sechellia* also increases the number of more elastic cells in the dorsal side of the embryo that participate in the invagination of a larger mesoderm. As in the case of pMAD, the ratio between *dpp* and *zen* shows a lack of scaling between these domains, with *D. sechellia* having a lower ratio than *D. melanogaster* and *D. simulans* (Figure 3f). We could not perform a similar analysis for *zen* in *D. busckii* due to failure in detecing specific signal in the dorsal midline for this gene.

When we analyzed *rho* and *pnr*, we noticed that the domains of these genes do not appear to scale in relation to the *dpp* domain. For instance, the number of cells expressing *rho* is the same across all species (~12 cells), regardless of how small or large their dorsal embryonic region is (Figure 3b,d). This result indicates that the domain immediately adjacent to *zen* does not scale with embryo size. In contrast, the absolute number of cells that express *pnr* varies across species, and this variation is also independent from the size of the dorsal region (Figure 3b,e). The more closely related species *D. simulans* and *D. sechellia* share a narrower *pnr* domain (25 and 27 cells) than the more distanly related *D. melanogaster* species (31 cells), suggesting that the border between elastic and rigid cells in the ectoderm has been moved more dorsally in comparison to *D. melanogaster*. The same is observed for *D. busckii*, which also has a narrower *pnr* domain (22 cells) than *D. melanogaster*. Finally, it is possible to estimate the number of cells in the ventral ectoderm that are exposed to low DPP levels by subtracting the number of cells that express *dpp* (Figure 1b) from those that express *pnr* (Figure 3e). This region is the smallest in *D. melanogaster* (~6 cells), followed by *D. busckii* (~10 cells), *D. simulans*, and *D. sechellia* (~13 cells).

The results above show that *zen*, *rho*, and *pnr* expression domains do not scale to embryo size or *dpp* domain, as clearly seen in the variable ratios obtained between *dpp* and its target domains (Figure 3f–h). Among the *melanogaster* sibling species, *D. simulans* shares some similarities with *D. melanogaster* (e.g., sizes of *dpp* and *zen* domains), and other similarities with *D. sechellia* (e.g., sizes of *pnr* and low DPP domains).

2.4 | Decreasing the concentration of the DPP antagonist short gastrulation (SOG) preferentially expands peak DPP activity levels

We hypothesize that the expansion of peak DPP levels (pMAD and *zen*) in *D. sechellia* could be due to a lowered concentration of SOG caused by its diffusion within a broader dorsal domain. SOG is secreted from the neuroectoderm and inhibits DPP signaling in the neuroectoderm and enhances it in the dorsal midline (Ashe & Levine, 1999; Biehs et al., 1996; Eldar et al., 2002; Francois et al., 1994; Mizutani et al., 2005; Shimmi et al., 2005). Removal of SOG causes a loss of peak DPP levels (Ashe & Levine, 1999), whereas decreasing its dosage in *sog* heterozygotes causes expansion in peak DPP levels characterized by expansion of the pMAD stripe (Mizutani et al., 2005) and the co-Smad protein Medea (Sutherland et al., 2003).

In *D. sechellia*, SOG must diffuse a longer distance within the dorsal region, which is expected to lower its overall concentration in this region. To test the hypothesis that an increased expression domain of *dpp* and lowered SOG concentration combine to create the unique DPP activity profile present in *D. sechellia*, we recreated the *D. sechellia* condition in *D. melanogaster* and analyzed the effects on *zen* and *rho* domains. We reasoned that double heterozygous embryos for *sog* and the intracellular DPP antagonist *brinker* (*brk*) would have lowered SOG concentration as well as a slightly expanded range of *dpp* expression caused by a decrease in *brk* levels. *brk* is expressed in the neuroectoderm and encodes a transcriptional repressor of DPP target genes. In *brk* mutants, *dpp* expression is expanded into the neuroectoderm, as BRK antagonizes DPP from auto-regulaton in lateral regions (Jaźwińska et al., 1999). We confirmed that in *sog brk* heterozygotes, *dpp* expression is expanded by about six cells in late blastoderm embryos at the expense of a reduction of three cells on each neuroectodermal band (Figure S1), and found that *zen* expands from 5 to 8 nucleis and *rho* from 11 to 13 nuclei, respectively (Figure 4). These mutant patterns are similar to the numbers observed in *D. sechellia* of 8 cells for *zen* and 12 for *rho* (Figure 3c,d). Notably, there is a disporportionate expansion of *zen* of 60% increase compared to only 18% increase of *rho* domain. Supporting our

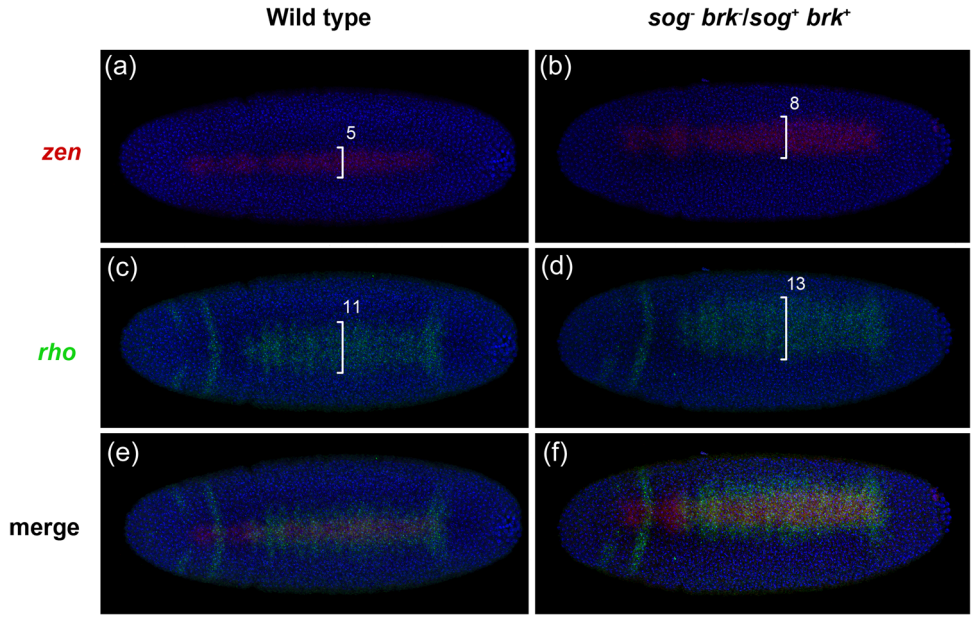

FIGURE 4 Reduction of short gastrulation and Decapentaplegic levels lead to nonproportional expansions of *zen* and *rho* domains. Comparison of *zen* (red) and *rho* (green) expression in wild-type (a,c,e) and *sog*-, *brk*- double heterozygotes (b,d,f) shows expanded domains in *sog*-, *brk*- heterozygotes from 5 to 8 *zen* cells and 11–13 *rho* cells (brackets in center of embryos). Anterior is to the left

hypothesis, these results suggest that decreasing the levels of SOG causes an expansion of peak levels of DPP activity, whereas high levels of DPP activity remain similar.

2.5 | Expansion of the dorsal embryonic region causes unscaled proportions in the expression domains of DPP-target genes

The results obtained from the *Drosophila* species and *sog brk* double heterozygotes indicate that the expression domains of genes regulated by DPP do not scale to size. To test how the DPP gradient would respond to a more extreme expansion of the dorsal embryonic region, we analyzed *zen*, *rho*, and *pnr* in dorsalized embryos. We used a heteroallelic combination of *spätzle* (spz^2 and spz^3 alleles) and *easter* (ea^{14} allele), two maternal mutations that decrease Toll activation and the levels of nuclear DL. spz^2 is an amorphic allele, and spz^3 and ea^{14} are temperature-sensitive hypomorphic alleles with reduced wild-type (WT) function at 25°C (Jin & Anderson, 1990; Morisato & Anderson, 1994). spz^2/spz^3ea^{14} mothers produce dorsalized embryos at 25°C with expanded *dpp* expression at the expense of the mesoderm (Figure S2). Nearly the entire span of the mesoderm (about 18 cells) is reduced in these mutants, whereas the neuroectoderm is left mostly intact with similar numbers of *sog* and *brk* expressing cells as in the WT (Figure S2). It is not known how the DPP-target gene domains are reorganized in these dorsalized embryos. One possibility is that the expression domains of *zen*, *rho*, and *pnr* expand in step with each other at the expense of the fates defined by low-DPP levels only. In this case, the ratios between *zen*, *rho*, and *pnr* would be similar to the wild-ype ratios. This finding would argue for the existence of a scaling mechanism for the DPP gradient in the embryo. Our results show that all three domains expand in the mutant (Figure 5a). However, their expansions are unequal. Specifically, the *zen* domain expands more than the *rho* and *pnr* domains (Figure 5b–d), and the *rho* domain expands more than the *pnr* domain (Figure 5d). These results indicate that the embryo lacks compensatory mechanisms for scaling of the DPP gradient, unlike in other developmental contexts where the DPP/BMP gradient is adjusted to size by an "expander" molecule (Ben-Zvi, Pyrowolakis, et al., 2011; Hamaratoglu et al., 2011; Mateus et al., 2020). We speculate that the lack of a scaling mechanism of the DPP gradient in the embryo may at least partly explain the DPP gradient shapes observed in the species with different embryo sizes. Indeed, the effects seen in dorsalized embryos above of more expansion of *zen* than *pnr* expression are similar to the changes observed in these domains in *D. sechellia*. However, one difference we note is that *rho* shows an expansion in dorsalized *D. melanogaster* embryos, but its expression domain is constant in all species.

3 | DISCUSSION

3.1 | There is no feedback mechanism that scales the DPP activity gradient in the embryo

Here we show that the specification of the entire DPP/BMP expression domain scales to embryo size of related *Drosophila*

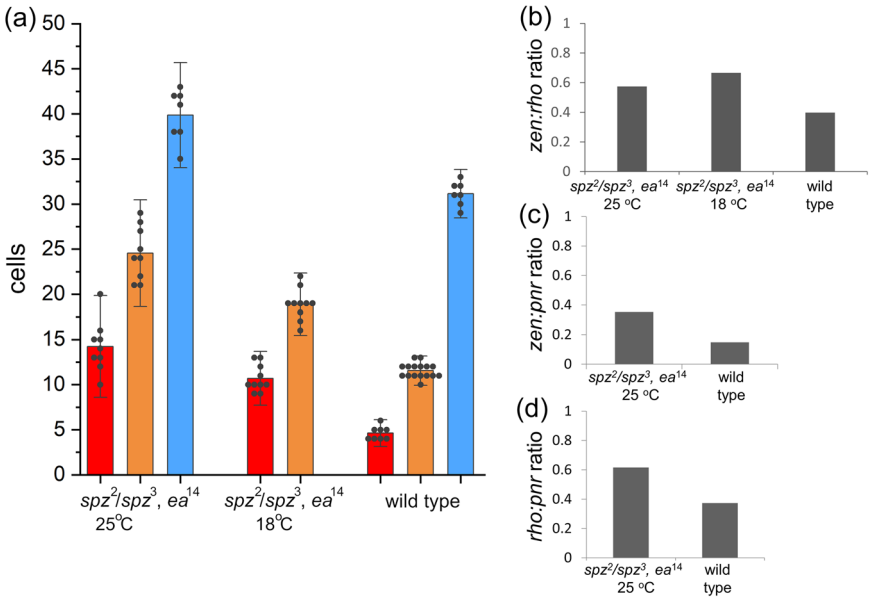

FIGURE 5 Alterations in the size of ectodermal domains lead to skewed expression domains of Decapentaplegic (DPP)-target genes. (a) *zen*, *rho*, and *pnr* expression widths in wild-type (WL) and expanded dorsal ectoderm embryos (spz^2/spz^3ea^{14}). Measurements for all three genes are shown for more extreme phenotype of expanded ectoderm in mutant embryos collected at 25°C; *zen* and *rho* are shown for milder phenotypes from embryos collected at 18°C. Error bars are 2 standard deviation in both directions. Scaling of DPP-target gene expression domains was determined by obtaining following ratios: (b) *zen:rho*, (c) *zen:pnr*, (d) *rho:pnr*. Note alterations in ratios between mutants and WL, including the *zen:rho* ratio obtained from spz^2/spz^3ea^{14} milder mutants collected at 18°C

species. This finding is in contrast to the other embryonic germ layers that either show disproportional sizes to total embryo size (i.e., the mesoderm) or that maintain a constant size and patterning during evolution (i.e., the neuroectoderm) (Belu & Mizutani, 2011; Chahda et al., 2013). Such scaling of the dorsal embryonic region is presumably driven by the DL gradient since DL defines the size of *dpp* expression domain by repressing *dpp* in ventral and lateral regions. However, although the entire dorsal region scales to embryo size, our analyses show that the scaling of pMAD across species and expression domain widths of DPP-target genes are not maintained during evolution. These findings indicate that the DPP activity gradient may have acquired unique shapes during evolution. Our results using mutations in *D. melanogaster* that cause an enlarged ectodermal size show that the DPP gradient lacks a mechanism of scaling in the embryo to generate proportional expression domains of DPP-target genes, which could in part explain the changes in the DPP gradient observed in the species.

In contrast to our findings in the embryo, the DPP gradient shows a great degree of scaling to size during wing growth and is particularly precise at maintaining proportional positions of wing veins. We conclude that it is unlikely that *pent/magu* also functions as a gradient expander to adjust the DPP gradient in the embryo when the ectodermal domain is increased. Although our results cannot ascertain the mechanisms behind the differential scaling of the DPP gradient across species, we speculate that the absence of an expander molecule in the embryo may partly explain the different DPP gradient shapes established within smaller or larger ectoderms.

3.2 | Disproportionate domains of DPP-target genes are expected to reorganize the distribution of cells with different mechanical properties required during gastrulation

We speculate that the evolutionary implication for the lack of scaling of the DPP gradient in the embryo is the generation and subsequent selection for new gene expression borders that define the amnioserosa and ectodermal domains, which can increase or decrease the number of cells with specific mechanical properties to support forces for the gastrulation of differently sized embryos. For instance, in comparison to *D. melanogaster*, the *pnr* border is shifted dorsally in *D. sechellia* and *D. simulans*. This change is expected to create a larger field of rigid cells in the lateral region of the embryo capable of generating stronger forces when these cells move ventrally, allowing for the invagination of the larger mesoderms observed in these two species. In addition, *D. sechellia*, the species with the largest egg size, has an increased *zen* domain, which is expected to specify more elastic cells and therefore allow more stretching in the dorsal region during invagination of the mesoderm. The additional amnioserosa cells in *D. sechellia* are also expected to generate stronger mechanical forces for moving a larger germ band. Those adaptions would explain the similar durations between gastrulation events seen in these three *melanogaster* subgroup species (Kuntz & Eisen, 2014). In *D. busckii*, which has a smaller mesoderm compared to *D. melanogaster*, the *pnr* border is also shifted dorsally (Belu & Mizutani, 2011). Because this species has small-sized cells less than half the size of *D. melanogaster* cells (Chahda et al., 2013), an increase in the number of rigid cells in

the lateral region may be necessary to achieve the necessary forces for the mesoderm invagination.

3.3 | DV patterning shows variations in mesoderm, ectoderm, and amnioserosa during evolution, but the neuroectoderm patterning remains robust

Our results presented here and in previous work suggest that patterning of ventral and dorsal regions of the embryo, which are established mainly by one gradient (i.e., either the DL or the DPP gradient) are more prone to have expansions and retractions of gene expression domains. Such changes in patterning are observed even within the *melanogaster* species subgroup that diverged very recently. In the case of the ventral region, direct measurements of nuclear DL levels showed that the DL gradient acquired different shapes during the evolution of Drosophilids (Ambrosi et al., 2014; Chahda et al., 2013). In contrast, in the lateral region of the embryo where the DL and DPP gradients overlap, the patterning of neuroectodermal domains remains highly conserved across divergent insect species. This finding agrees with models of scale-invariance in cellular fields patterned by opposing gradients (McHale et al., 2006). Indeed, we find that the neuroectoderm patterning remains very robust against the changes in the DPP and DL activity gradients in $spz^{3}ea^{14}/spz^{3}ea^{14}$ mutants. In these embryos, the neural identity genes *vnd*, *ind*, and *Drop/msh* (Isshiki et al., 1997; Jimenez et al., 1995; McDonald et al., 1998; Mellerick & Nirenberg, 1995; von Ohlen & Doe, 2000; Weiss et al., 1998) subdomains are only slightly distorted at either 18°C or 25°C (Figure S2) in contrast to the much stronger effects of nearly elimination of the mesoderm and expansion of the dorsal region with a lack of scaling among DPP-target expression domains. Thus, the available data on DV patterning in these species suggest that the gene expression domain sizes in the ventral mesoderm and dorsal regions are fast evolving. One reason for the changes in the expression patterns is the modified shapes of the DPP and DL gradients in these species. Another reason that remains to be tested is the actual interpretation of the gradients at the level of the target gene enhancers. Our study cannot predict how individual or multiple enhancers for a single target gene may respond to not only DPP, but also DL, and receive additional regulatory inputs from other DV factors. For instance, *zen* is activated by DPP but it also contains a ventral repressor element that is regulated by DL in dorsal regions of the embryo (Cai et al., 1996; Valentine et al., 1998). Another example is *rho*, which is regulated by DPP as well as DL through the lateral stripe enhancer element NEE (Cai et al., 1996; Ip et al., 1992). The fact that *rho* receives input from both gradients, and not only DPP, could explain why its domain remains restricted to a similar size across species. Future studies could also test the effect of redundancy in the response to DPP gradient alone afforded by shadow enhancers (Hong et al., 2008), which have higher divergent rates within *Drosophila* species and are likely to have been modified during evolution.

In conclusion, the differential scaling of DV gene expression domains described in this study seems critical to accommodate a neuroectoderm of fixed size that preserves neuronal lineage specification. Furthermore, the results presented here suggest that expansions or retractions of amnioserosa and ectodermal domains containing cells with different mechanical properties may contribute to creating variable strengths in the mechanical forces required for the gastrulation of larger or smaller embryos.

4 | MATERIALS AND METHODS

4.1 | Fly stocks and genetic crosses

*y w D. melanogaster*was used as WT. The following stocks from the National Drosophila Species Stock Center (currently at the Cornell College of Agriculture and Life Science) were used: *D. busckii* (WT), *D. simulans* (WT), and *D. sechellia* ($zn^{1}v^{1}f,^{1}$). The following *D. melanogaster* stocks were obtained from the Bloomington Drosophila Stock Center: ($spz^{2}ca^{1}$/TM1, #3115), ($ru^{1}st^{1}ea^{14}spz^{3}ca^{1}$/TM1, #3287). $spz^{2}ca^{1}$/TM1 flies were crossed to $ru^{1}st^{1}ea^{14}spz^{3}ca^{1}$/TM1 and $spz^{2}ca^{1}/ru^{1}st^{1}ea^{14}spz^{3}ca^{1}$ females were selected. The *D. melanogaster* $sog,^{y506}$ brk^{m68}/FM7 stock was used to produce *sog*-, *brk*- heterozygote female embryos. *sog*-, *brk*- heterozygote female embryos were genotyped by triple FISH for *sog*, *rho*, *zen*, and identified as embryos with a single nuclear nascent transcript for *sog* and altered domain sizes for *rho* and *zen* in the ectoderm.

4.2 | Immunohistochemistry and confocal imaging

Embryos were collected for 5–6 h at 18°C or 25°C in grape juice agar plates supplemented with yeast (or noni fruit leather for *D. sechellia*), fixed, and processed for in situ and protein staining as described in (Kosman et al., 2004). Probes against *zen*, *race*, *rho*, *pnr*, *vnd*, *ind*, and *msh* were labeled with either digoxigenin (DIG; Roche), biotin (Bio; Roche) or dinitrophenol (DNP; PerkinElmer). Primary antibodies and dilutions used were: sheep anti-DIG (1:1000; Roche), mouse anti-Bio (1:1000; Roche), rabbit anti-DNP (1:2000; Invitrogen), and rabbit anti-Smad3 (1:100; Abcam). Secondary antibodies were used at a 1:500 concentration: donkey anti-sheep Alexa 488, donkey anti-rabbit Alexa 555, and donkey anti-mouse Alexa 647 (Invitrogen). Nuclei were stained with DAPI (Invitrogen) at 300 nM for 15 min. Embryos were mounted in SlowFade (Life Technologies) and imaged in a Zeiss LSM700 Confocal. Gain and offset settings were adjusted to nonsaturating levels spanning entire 12-bit dynamic range. Images were exported to ImageJ and Axiovision (Zeiss) for data analysis.

4.3 | Statistics

Statistical analyses were performed using the PAST software (version 2.09, http://folk.uio.no/ohammer/past/). The data were compared

using one-way analysis of variance (ANOVA), followed by Tukey's test for pairwise comparison. The cutoff used for statistical significance was $p < 0.05$.

ACKNOWLEDGMENTS

We thank the anonymous reviewers for their comments to improve this manuscript. This study was initially supported by a grant from the National Science Foundation (IOS-1051662), and grants from the National Institutes of Health (R21EB016535, R33AG049863) to C. M. M. J. S. C. was supported by the CWRU College of Arts and Sciences and a GAANN PhD training grant from the US Department of Education. P. A. was supported by CAPES/Brasilia fellowship under Brazil Science without Borders program.

CONFLICTS OF INTEREST

The authors declare no conflicts of interest.

DATA AVAILABILITY STATEMENT

The data that support the findings of this study are available from the corresponding author upon reasonable request.

REFERENCES

Ambrosi, P., Chahda, J. S., Koslen, H. R., Chiel, H. J., & Mizutani, C. M. (2014). Modeling of the dorsal gradient across species reveals interaction between embryo morphology and Toll signaling pathway during evolution. *PLoS Computational Biology*, *10*(8), e1003807. https://doi.org/10.1371/journal.pcbi.1003807

Ashe, H. L., & Levine, M. (1999). Local inhibition and long-range enhancement of Dpp signal transduction by Sog. *Nature*, *398*(6726), 427–431. https://doi.org/10.1038/18892

Ashe, H. L., Mannervik, M., & Levine, M. (2000). Dpp signaling thresholds in the dorsal ectoderm of the *Drosophila* embryo. *Development*, *127*(15), 3305–3312.

Belu, M., & Mizutani, C. M. (2011). Variation in mesoderm specification across Drosophilids is compensated by different rates of myoblast fusion during body wall musculature development. *PLoS One*, *6*(12), e28970. https://doi.org/10.1371/journal.pone.0028970

Ben-Zvi, D., Pyrowolakis, G., Barkai, N., & Shilo, B. -Z. (2011). Expansion-repression mechanism for scaling the Dpp activation gradient in *Drosophila* wing imaginal discs. *Current Biology: CB*, *21*(16), 1391–1396. https://doi.org/10.1016/j.cub.2011.07.015

Ben-Zvi, D., Shilo, B. Z., & Barkai, N. (2011). Scaling of morphogen gradients. *Current Opinion in Genetics & Development*, *21*(6), 1–7. https://doi.org/10.1016/j.gde.2011.07.011

Ben-Zvi, D., Shilo, B. Z., Fainsod, A., & Barkai, N. (2008). Scaling of the BMP activation gradient in *Xenopus* embryos. *Nature*, *453*(7199), 1205–1211. https://doi.org/10.1038/nature07059

Biehs, B., François, V., & Bier, E. (1996). The *Drosophila* short gastrulation gene prevents Dpp from autoactivating and suppressing neurogenesis in the neuroectoderm. *Genes & Development*, *10*(22), 2922–2934.

Bier, E., Jan, L. Y., & Jan, Y. N. (1990). Rhomboid, a gene required for dorsoventral axis establishment and peripheral nervous system development in *Drosophila melanogaster*. *Genes & Development*, *4*(2), 190–203.

Butler, L. C., Blanchard, G. B., Kabla, A. J., Lawrence, N. J., Welchman, D. P., Mahadevan, L., Adams, R. J., & Sanson, B. (2009). Cell shape changes indicate a role for extrinsic tensile forces in *Drosophila* germ-band extension. *Nature Cell Biology*, *11*(7), 859–864. https://doi.org/10.1038/ncb1894

Cai, H. N., Arnosti, D. N., & Levine, M. (1996). Long-range repression in the *Drosophila* embryo. *Proceedings of the National Academy of Sciences*, *93*(18), 9309–9314. https://doi.org/10.1073/pnas.93.18.9309

Chahda, J. S., Sousa-Neves, R., & Mizutani, C. M. (2013). Variation in the dorsal gradient distribution is a source for modified scaling of germ layers in *Drosophila*. *Current Biology*, *23*(8), 710–716. https://doi.org/10.1016/j.cub.2013.03.031

Crocker, J., Tamori, Y., & Erives, A. (2008). Evolution acts on enhancer organization to fine-tune gradient threshold readouts. *PLoS Biology*, *6*(11), e263. https://doi.org/10.1371/journal.pbio.0060263

David, J. R., Lemeunier, F., Tsacas, L., & Yassin, A. (2007). The historical discovery of the nine species in the *Drosophila melanogaster* species subgroup. *Genetics*, *177*(4), 1969–1973. https://doi.org/10.1534/genetics.104.84756

Doe, C. Q. (1992). Molecular markers for identified neuroblasts and ganglion mother cells in the *Drosophila* central nervous system. *Development*, *116*(4), 855–863.

Dorfman, R., & Shilo, B. Z. (2001). Biphasic activation of the BMP pathway patterns the *Drosophila* embryonic dorsal region. *Development*, *128*(6), 965–972.

Eldar, A., Dorfman, R., Weiss, D., Ashe, H., Shilo, B. -Z., & Barkai, N. (2002). Robustness of the BMP morphogen gradient in *Drosophila* embryonic patterning. *Nature*, *419*(6904), 304–308. https://doi.org/10.1038/nature01061

Francois, V., Solloway, M., O'Neill, J. W., Emery, J., & Bier, E. (1994). Dorsal-ventral patterning of the *Drosophila* embryo depends on a putative negative growth factor encoded by the short gastrulation gene. *Genes & Development*, *8*(21), 2602–2616.

Garcia, M., Nahmad, M., Reeves, G. T., & Stathopoulos, A. (2013). Size-dependent regulation of dorsal-ventral patterning in the early *Drosophila* embryo. *Developmental Biology*, *381*(1), 286–299. https://doi.org/10.1016/j.ydbio.2013.06.020

Gorfinkiel, N., Schamberg, S., & Blanchard, G. B. (2011). Integrative approaches to morphogenesis: Lessons from dorsal closure. *Genesis*, *49*(7), 522–533. https://doi.org/10.1002/dvg.20704

Graveley, B. R., Brooks, A. N., Carlson, J. W., Duff, M. O., Landolin, J. M., Yang, L., Artieri, C. G., van Baren, M. J., Boley, N., Booth, B. W., Brown, J. B., Cherbas, L., Davis, C. A., Dobin, A., Li, R., Lin, W., Malone, J. H., Mattiuzzo, N. R., Miller, D., & Celniker, S. E. (2011). The developmental transcriptome of *Drosophila melanogaster*. *Nature*, *471*(7339), 473–479. https://doi.org/10.1038/nature09715

Gregor, T., Bialek, W., de Ruyter van Steveninck, R. R., Tank, D. W., & Wieschaus, E. F. (2005). Diffusion and scaling during early embryonic pattern formation. *Proceedings of the National Academy of Sciences of the United States of America*, *102*(51), 18403–18407. https://doi.org/10.1073/pnas.0509483102

Hamaratoglu, F., de Lachapelle, A. M., Pyrowolakis, G., Bergmann, S., & Affolter, M. (2011). Dpp signaling activity requires Pentagone to scale with tissue size in the growing *Drosophila* wing imaginal disc. *PLoS Biology*, *9*(10), e1001182. https://doi.org/10.1371/journal.pbio.1001182

Hong, J. W., Hendrix, D. A, Papatsenko, D., & Levine, M. S. (2008). How the dorsal gradient works: Insights from postgenome technologies. *Proceedings of the National Academy of Sciences of the United States of America*, *105*(51), 20072–20076.

Huang, Y., & Umulis, D. M. (2019). Scale invariance of BMP signaling gradients in zebrafish. *Scientific Reports*, *9*(1). https://doi.org/10.1038/s41598-019-41840-8

Ip, Y. T., Park, R. E., Kosman, D., Bier, E., & Levine, M. (1992). The dorsal gradient morphogen regulates stripes of rhomboid expression in the presumptive neuroectoderm of the *Drosophila* embryo. *Genes & Development*, *6*(9), 1728–1739. https://doi.org/10.1101/gad.6.9.1728

Isshiki, T., Takeichi, M., & Nose, A. (1997). The role of the msh homeobox gene during *Drosophila* neurogenesis: Implication for the dorsoventral specification of the neuroectoderm. *Development*, *124*(16), 3099–3109.

Jaźwińska, A., Rushlow, C., & Roth, S. (1999). The role of brinker in mediating the graded response to Dpp in early *Drosophila* embryos. *Development*, *126*(15), 3323–3334.

Jimenez, F., Martin-Morris, L. E., Velasco, L., Chu, H., Sierra, J., Rosen, D. R., & White, K. (1995). vnd, a gene required for early neurogenesis of *Drosophila*, encodes a homeodomain protein. *EMBO Journal*, *14*(14), 3487–3495.

Jin, Y. S., & Anderson, K. V. (1990). Dominant and recessive alleles of the *Drosophila* easter gene are point mutations at conserved sites in the serine protease catalytic domain. *Cell*, *60*(5), 873–881.

Kong, D., Wolf, F., & Großhans, J. (2017). Forces directing germ-band extension in *Drosophila* embryos. *Mechanisms of Development*, *144*, 11–22. https://doi.org/10.1016/j.mod.2016.12.001

Kosman, D., Mizutani, C. M., Lemons, D., Cox, W. G., McGinnis, W., & Bier, E. (2004). Multiplex detection of RNA expression in *Drosophila* embryos. *Science*, *305*(5685), 846.

Kuntz, S. G., & Eisen, M. B. (2014). *Drosophila* embryogenesis scales uniformly across temperature in developmentally diverse species. *PLoS Genetics*, *10*(4), e1004293. https://doi.org/10.1371/journal.pgen.1004293

Lachaise, D., David, J. R., Lemeunier, F., Tsacas, L., & Ashburner, M. (1986). The reproductive relationships of *Drosophila sechellia* with *D. mauritiana*, *D. simulans*, and *D. melanogaster* from the Afrotropical region. *Evolution*, *40*(2), 262–271.

Lacy, M. E., & Hutson, M. S. (2016). Amnioserosa development and function in *Drosophila* embryogenesis: Critical mechanical roles for an extraembryonic tissue. *Developmental Dynamics*, *245*(5), 558–568. https://doi.org/10.1002/dvdy.24395

Lott, S. E., Kreitman, M., Palsson, A., Alekseeva, E., & Ludwig, M. Z. (2007). Canalization of segmentation and its evolution in *Drosophila*. *Proceedings of the National Academy of Sciences of the United States of America*, *104*(26), 10926–10931. https://doi.org/10.1073/pnas.0701359104

Maduzia, L. L., & Padgett, R. W. (1997). *Drosophila* MAD, a member of the Smad family, translocates to the nucleus upon stimulation of the dpp pathway. *Biochemical and Biophysical Research Communications*, *238*(2), 595–598. https://doi.org/10.1006/bbrc.1997.7353

Markow, T. A., Beall, S., & Matzkin, L. M. (2009). Egg size, embryonic development time and ovoviviparity in *Drosophila* species. *Journal of Evolutionary Biology*, *22*(2), 430–434.

Mateus, R., Holtzer, L., Seum, C., Hadjivasiliou, Z., Dubois, M., Jülicher, F., & Gonzalez-Gaitan, M. (2020). BMP Signaling gradient scaling in the Zebrafish pectoral fin. *Cell Reports*, *30*(12), 4292–4302e7. https://doi.org/10.1016/j.celrep.2020.03.024

McDonald, J. A., Holbrook, S., Isshiki, T., Weiss, J., Doe, C. Q., & Mellerick, D. M. (1998). Dorsoventral patterning in the *Drosophila* central nervous system: The vnd homeobox gene specifies ventral column identity. *Genes and Development*, *12*(22), 3603–3612.

McHale, P., Rappel, W. J., & Levine, H. (2006). Embryonic pattern scaling achieved by oppositely directed morphogen gradients. *Physical Biology*, *3*(2), 107–120. https://doi.org/10.1088/1478-3975/3/2/003

Mellerick, D. M., & Nirenberg, M. (1995). Dorsal-ventral patterning genes restrict NK-2 homeobox gene expression to the ventral half of the central nervous system of *Drosophila* embryos. *Developmental Biology*, *171*(2), 306–316. https://doi.org/10.1006/dbio.1995.1283

Mizutani, C. M., & Bier, E. (2008). EvoD/Vo: The origins of BMP signalling in the neuroectoderm. *Nature Reviews Genetics*, *9*(9), 663–677.

Mizutani, C. M., Meyer, N., Roelink, H., & Bier, E. (2006). Threshold-dependent BMP-mediated repression: A model for a conserved mechanism that patterns the neuroectoderm. *PLoS Biology*, *4*(10), e313. https://doi.org/10.1371/journal.pbio.0040313

Mizutani, C. M., Nie, Q., Wan, F. Y., Zhang, Y. T., Vilmos, P., Sousa-Neves, R., Bier, E., Marsh, J. L., & Lander, A. D. (2005). Formation of the BMP activity gradient in the *Drosophila* embryo. *Developmental Cell*, *8*(6), 915–924.

Morisato, D., & Anderson, K. (1994). The spätzle gene encodes a component of the extracellular signaling pathway establishing the dorsal-ventral pattern of the *Drosophila* embryo. *Cell*, *76*, 677–688.

Newfeld, S. J., Chartoff, E. H., Graff, J. M., Melton, D. A., & Gelbart, W. M. (1996). Mothers against dpp encodes a conserved cytoplasmic protein required in DPP/TGF-beta responsive cells. *Development*, *122*(7), 2099–2108.

Raftery, L. A, & Sutherland, D. J. (1999). TGF-beta family signal transduction in *Drosophila* development: From Mad to Smads. *Developmental Biology*, *210*(2), 251–268. https://doi.org/10.1006/dbio.1999.9282

Rauzi, M., Krzic, U., Saunders, T. E., Krajnc, M., Ziherl, P., Hufnagel, L., & Leptin, M. (2015). Embryo-scale tissue mechanics during *Drosophila* gastrulation movements. *Nature Communications*, *6*(1), 8677. https://doi.org/10.1038/ncomms9677

Reeves, G. T., & Stathopoulos, A. (2009). Graded dorsal and differential gene regulation in the *Drosophila* embryo. *Cold Spring Harbor Perspectives in Biology*, *1*(4), a000836. https://doi.org/10.1101/cshperspect.a000836

Rushlow, C., Colosimo, P. F., Lin, M. C., Xu, M., & Kirov, N. (2001). Transcriptional regulation of the *Drosophila* gene zen by competing Smad and Brinker inputs. *Genes & Development*, *15*(3), 340–351. https://doi.org/10.1101/gad.861401

Schloop, A. E., Bandodkar, P. U., & Reeves, G. T. (2020). Formation, interpretation, and regulation of the *Drosophila* Dorsal/NF-κB gradient. *Gradients and Tissue Patterning*, 143–191. https://doi.org/10.1016/bs.ctdb.2019.11.007

Shimmi, O., Umulis, D., Othmer, H., & O′Connor, M. B. (2005). Facilitated transport of a Dpp/Scw heterodimer by Sog/Tsg leads to robust patterning of the *Drosophila* blastoderm embryo. *Cell*, *120*(6), 873–886. https://doi.org/10.1016/j.cell.2005.02.009

Stathopoulos, A., & Levine, M. (2002). Dorsal gradient networks in the *Drosophila* embryo. *Developmental Biology*, *246*(1), 57–67. https://doi.org/10.1006/dbio.2002.0652

Stathopoulos, A., & Levine, M. (2005). Genomic regulatory networks and animal development. *Developmental Cell*, *9*(4), 449–462. https://doi.org/10.1016/j.devcel.2005.09.005

Sutherland, D. J., Li, M., Liu, X. Q., Stefancsik, R., & Raftery, L. A. (2003). Stepwise formation of a SMAD activity gradient during dorsal-ventral patterning of the *Drosophila* embryo. *Development*, *130*(23), 5705–5716. https://doi.org/10.1242/dev.00801

Tamura, K., Subramanian, S., & Kumar, S. (2004). Temporal patterns of fruit fly (*Drosophila*) evolution revealed by mutation clocks. *Molecular Biology and Evolution*, *21*(1), 36–44.

Thomas, J. B., Bastiani, M. J., Bate, M., & Goodman, C. S. (1984). From grasshopper to *Drosophila*: A common plan for neuronal development. *Nature*, *310*(5974), 203–207.

Umulis, D. M., Shimmi, O., O′Connor, M. B., & Othmer, H. G. (2010). Organism-scale modeling of early *Drosophila* patterning via bone morphogenetic proteins. *Developmental Cell*, *18*(2), 260–274. https://doi.org/10.1016/j.devcel.2010.01.006

Valentine, S. A., Chen, G., Shandala, T., Fernandez, J., Mische, S., Saint, R., & Courey, A. J. (1998). Dorsal-mediated repression requires the formation of a multiprotein repression complex at the ventral silencer. *Molecular and Cellular Biology*, *18*(11), 6584–6594. https://doi.org/10.1128/mcb.18.11.6584

von Ohlen, T., & Doe, C. Q. (2000). Convergence of dorsal, dpp, and egfr signaling pathways subdivides the *Drosophila* neuroectoderm into three dorsal-ventral columns. *Developmental Biology*, *224*(2),

362–372. https://doi.org/10.1006/dbio.2000.9789S0012-1606(00)99789-6

Weiss, J. B., Von Ohlen, T., Mellerick, D. M., Dressler, G., Doe, C. Q., & Scott, M. P. (1998). Dorsoventral patterning in the *Drosophila* central nervous system: The intermediate neuroblasts defective homeobox gene specifies intermediate column identity. *Genes and Development*, *12*(22), 3591–3602.

Whitington, P. (1996). Evolution of neural development in the arthropods. *Seminars in Cell & Developmental Biology*, *7*(4), 605–614.

Winick, J., Abel, T., Leonard, M. W., Michelson, A. M., Chardon-Loriaux, I., Holmgren, R. A., Maniatis, T., & Engel, J. D. (1993). A GATA family transcription factor is expressed along the embryonic dorsoventral axis in *Drosophila melanogaster*. *Development*, *119*(4), 1055–1065.

Wotton, D., & Massagué, J. (2001). Smad transcriptional corepressors in TGF beta family signaling. *Current Topics in Microbiology and Immunology*, *254*, 145–164.

SUPPORTING INFORMATION

Additional supporting information can be found online in the Supporting Information section at the end of this article.

How to cite this article: Chahda, J. S., Ambrosi, P., & Mizutani, C. M. (2023). The nested embryonic dorsal domains of BMP-target genes are not scaled to size during the evolution of *Drosophila* species. *Journal of Experimental Zoology Part B: Molecular and Developmental Evolution*, 340, 131–142. https://doi.org/10.1002/jez.b.23137